LAWRENCE
LIVERMORE
NATIONAL
LABORATORY

LLNL-CONF-401454

Decomposition of the Multistatic Response Matrix and Target Characterization

D. H. Chambers

February 19, 2008

XXIXth URSI General Assembly
Chicago, IL, United States
August 9, 2008 through August 16, 2008

Disclaimer

Decomposition of the Multistatic Response Matrix and Target Characterization

D. H. Chambers

Lawrence Livermore National Laboratory, PO Box 808 L-154, Livermore, CA. chambers2@llnl.gov

Abstract

Decomposition of the time-reversal operator for an array, or equivalently the singular value decomposition of the multistatic response matrix, has been used to improve imaging and localization of targets in complicated media. Typically, each singular value is associated with one scatterer even though it has been shown in several cases that a single scatterer can generate several singular values. In this paper we review the analysis of the time-reversal operator (TRO), or equivalently the multistatic response matrix (MRM), of an array system and a small target. We begin with two-dimensional scattering from a small cylinder then show the results for a small non-spherical target in three dimensions. We show that the number and magnitudes of the singular values contain information about target composition, shape, and orientation.

1. Small cylindrical targets

Consider the case of a linear array of short dipole elements with total length L, and a small cylinder of radius a placed a distance y_a from the array (see Fig. 1). The far field magnetic and electric fields radiated from the nth array element are

$$\begin{aligned} \mathbf{H}_n(x,y) &= -\frac{d}{2} I_n \sqrt{\frac{k}{2\pi i R_n}} e^{ikR_N} \hat{\mathbf{R}}_n \times \hat{\mathbf{e}}_x \,, \\ \mathbf{E}_n(x,y) &= -\frac{1}{\varepsilon_0 c} \hat{\mathbf{R}}_n \times \mathbf{H}_n(x,y) \,, \end{aligned} \tag{1}$$

where c is the speed of light, d is the length of the dipole elements, ε_0 is the electrical permittivity of free space, and $\mathbf{R}_n = \mathbf{r} - \mathbf{r}_n$. The position of the nth element is given by the vector $\mathbf{r}_n = (\xi_n, -y_a, 0)$, with magnitude r_n and unit direction vector $\hat{\mathbf{r}}_n$. The vector $\mathbf{r} = (x, y, 0)$ is the field point. The scalar R_n is the magnitude of the vector $\mathbf{R}_n$ and $\hat{\mathbf{R}}_\mathbf{n}$ is the unit vector in the direction of $\mathbf{R}_n$. The dipole element is oriented parallel to the x axis (unit vector $\hat{\mathbf{e}}_x$) and is driven by the current I_n.

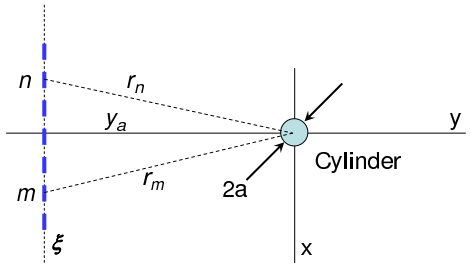

Figure 1. Linear array of short dipole elements, total length L, and a small cylinder of radius a. The distance between the cylinder and array is y_a.

For a thin cylinder (or wire) of radius $a \ll z_a$ centered at the origin, the field incident on the cylinder from the *nth* element can be approximated as a plane wave coming from the direction of the element. The field scattered from an incident plane wave is given to leading order (far-field) by

$$\mathbf{E}^{(s)}(x,y) = \sqrt{\frac{2}{i\pi kr}} e^{ikr} \left[\hat{\mathbf{r}} \times (\mathbf{m} + \hat{\mathbf{r}} \times \mathbf{p})\right] \,, \tag{2}$$

where $\mathbf{p}$ is the induced electric dipole moment and $\mathbf{m}$ is the induced magnetic dipole moment generated by the incident field. The moments are related to the incident field $\mathbf{E}_n^{(i)}$ evaluated at the position of the cylinder $\mathbf{r} = 0$ ($\mathbf{R}_n = -\mathbf{r}_n$): $\mathbf{m} = -m_0 a^2\, \hat{\mathbf{r}}_n \times \mathbf{E}_n^{(i)}(-\mathbf{r}_n)$, $\mathbf{p} = p_0 a^2\, \mathbf{E}_n^{(i)}(-\mathbf{r}_n)$. The coefficients p_0 and m_0 determine the strengths of the induced moments and depend on frequency (f), relative permitivity (ε), permeability, and conductivity (σ) of the cylinder materal. For the pure dielectric ($\sigma = 0$), the magnetic moment vanishes and the electric dipole strength is $p_0 = 2(\varepsilon - 1)/(\varepsilon + 1)$. For the perfect electrical conductor (PEC, $\sigma \to \infty$), both electric and magnetic moments are present, with $p_0 = 2$ and $m_0 = -1$.

The scattered field is received by the array, where it induces a voltage on each dipole element. The voltages induced on the dipoles of the mth element can be expressed as

$$V_m = d\,[\hat{\mathbf{r}}_m \times (\hat{\mathbf{r}}_m \times \hat{\mathbf{e}}_\mathbf{x})] \cdot \mathbf{E}^{(s)}(\mathbf{r}_m) = -d\,\hat{\mathbf{e}}_\mathbf{x} \cdot \mathbf{E}^{(s)}(\mathbf{r}_m)\,, \tag{3}$$

Combining this with the previous expressions for the incident field (1) and scattered field (2) we find $V_m = K_{mn} I_n$, where

$$\begin{aligned} K_{mn} &= \frac{(ka)^2 d^2 q}{8\varepsilon_0 c} e^{ik(r_m + r_n)} \hat{K}_{mn}\,, \\ \hat{K}_{mn} &= -\frac{1}{q\sqrt{r_m r_n}} \left\{ p_0 \left[(\hat{\xi}_m^2 - 1)(\hat{\xi}_n^2 - 1) + \hat{\xi}_m \hat{\eta}_m \hat{\xi}_n \hat{\eta}_n \right] - m_0 \hat{\eta}_m \hat{\eta}_n \right\}\,. \end{aligned} \tag{4}$$

K_{mn} is an element of the MRM for the array and has units of impedance since it relates a current I_n to a voltage V_m. q is the combined magnitude of the dipole strengths, $q = \sqrt{|p_0|^2 + |m_0|^2}$, while $\hat{\xi}_m$ and $\hat{\eta}_m$ are equal to ξ_m/r_m and $-y_a/r_m$, respectively. The entire array response can be written $\mathbf{V} = \mathbf{K}\,\mathbf{I}$, where $\mathbf{I}$ is the vector of transmit currents for all the elements, and $\mathbf{V}$ is the vector of received voltages. The matrix $\mathbf{K}$ has the form of the sum of three outer products of vectors, two associated with the electric dipole moment and one with the magnetic dipole moment. In the most general case, the rank of $\mathbf{K}$ will be three and the SVD have three nonzero singular values[1, 4]. When the conductivity of the cylinder is negligible, the induced magnetic dipole moment is zero and there are only two singular values. Figure 2 shows the singular vectors and the singular values for a symmetric array and cylinder as a function of nondimensional range. The larger singular value is associated with an induced electric dipole aligned with the x axis. The smaller singular value is associated with a dipole aligned with the y axis. The orthogonality of the induced dipole moments are a consequence of the orthogonality of the singular vectors on the array. For a conducting cylinder, both electric and magnetic dipoles contribute to the scattered field to leading order, creating three singular values and singular vectors (Fig. 2).

From the analysis of the linear array and small cylinder, we see that the scattered field is produced by electric and magnetic dipole moments induced by the incident field. In this two-dimensional example, the scattered field is produced by an induced electric dipole moment in the xy plane (two component vector, 2 degrees of freedom), and induced magnetic dipole moment is in the z direction (single component, single degree of freedom). The maximum number of singular values of three, which occurs for the perfectly conducting cylinder, is determined by the three degrees of freedom represented by the induced dipole moments. For a dielectric cylinder, only the electric dipole moment is present, reducing the number of singular values to two. From this we can expect that in three dimensions there can be up to six singular values, three associated with the induced electric dipole moment, and three associated with the induced magnetic dipole moment. A PEC target could have six singular values, while a pure dielectric target would have a maximum of three.

2. Small targets in three dimensions

In three dimensions we can perform the same analysis using the appropriate equations for the field emitted from an array of crossed infinitesimal dipoles (Figure 3). Under the same assumptions as before, the scattered field to leading order ($\mathcal{O}((ka)^3)$) is[2, 3]

$$\mathbf{E}^{(s)}(\mathbf{r}) = -\frac{k^2 e^{ikr}}{r} \left[\hat{\mathbf{r}} \times (\mathbf{m} + \hat{\mathbf{r}} \times \mathbf{p}) \right]\,, \tag{5}$$

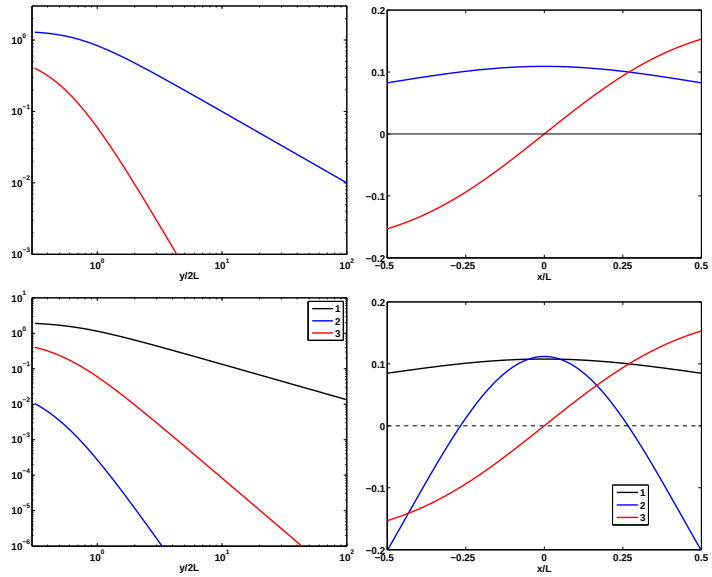

Figure 2. Singular values for a dielectric cylinder as a function of $L/2y_a$ (upper left). Amplitude of singular vectors for $L/2y_a = 1$ (upper right). Singular values for a conducting cylinder as a function of $L/2y_a$ (lower left). Amplitude of singular vectors for $L/2y_a = 1$ (lower right).

where $\mathbf{p}$ and $\mathbf{m}$ are the induced electric and magnetic dipole moments. For a small object of arbitrary shape the induced moments are related to the incident fields at the object through the electric ($\mathbf{D^e}$) and magnetic ($\mathbf{D^h}$) dipole tensors [2, 3]: $\mathbf{m} = \frac{1}{\varepsilon_0 c}\mathbf{D^h} \cdot \mathbf{H}_n^{(i)}$, $\mathbf{p} = \mathbf{D^e} \cdot \mathbf{E}_n^{(i)}$. The tensors themselves depend on the shape, size, and electromagnetic material properties (permittivity, permeability, conductivity) of the target. From these we can derive analytical expressions for the MRM and perform the SVD in the same way as we did for the cylinder (see Chambers and Berryman[5]).

Consider the case for a thin PEC disk ($a_1 = a_2 \gg a_3$). To leading order the dipole tensors are

$$\mathbf{D^e} = \frac{4a_1^3}{3\pi}\left(\mathbf{b}_1^T\,\mathbf{b}_1 + \mathbf{b}_2^T\,\mathbf{b}_2\right)\,, \qquad \mathbf{D^h} = \frac{2a_1^3}{3\pi}\,\mathbf{b}_3^T\,\mathbf{b}_3\,, \tag{6}$$

where $\mathbf{b}_3$ defines the axis perpendicular to the disk, and $\mathbf{b}_1$ and $\mathbf{b}_2$ are unit vectors in plane of the disk. Figure 4 shows the three singular values as functions of the disk orientation angles θ and ϕ for a symmetric linear array that has been rotated an angle ϕ' from the ξ axis. The ratio of array length to range is $L/z_a = 1$. We see that the first singular value is maximum when the array is aligned with the projection of the disk axis in the xy plane ($\phi - \phi' = 0$ or $\phi - \phi' = \pi$). The second singular value is maximum when the disk axis is perpendicular to the array. The behavior of the third singular value with ϕ is similar to the first. Fig. 28 also shows the behavior of the singular values with the pitch angle θ. The first singular value increases with pitch while the second and third decrease with pitch. This suggests that the pitch angle might be estimated by moving the array in a direction perpendicular to the array axis and tracking the change in the ratio of the first and second singular value. This implies that time-reversal imaging techniques might be constructed to extract the additional target information contained in multiple singular values.

Acknowledgements

This document was prepared as an account of work sponsored by an agency of the United States government. Neither the United States government nor Lawrence Livermore National Security, LLC, nor any of their employees makes any warranty, expressed or implied, or assumes any legal liability or responsibility for the accuracy, completeness, or usefulness of any information, apparatus, product, or process disclosed, or represents that its use would not infringe privately owned rights. Reference herein to any specific commercial product, process, or service by trade name, trademark, manufacturer, or otherwise does not necessarily constitute or imply its endorsement, recommen-

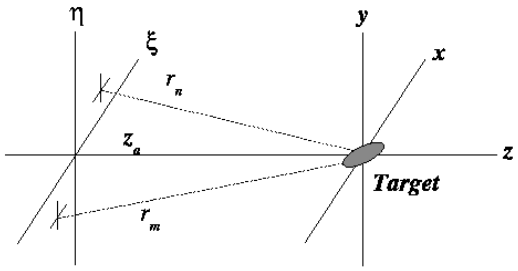

Figure 3. Planar array of short crossed dipole elements with a small ellipsoid placed a distance z_a from the plane of the array.

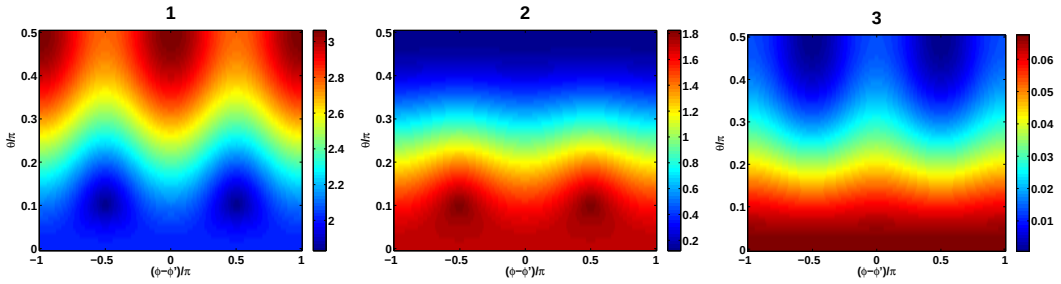

Figure 4. Three singular values for a linear array ($d_x = d_y$) rotated an angle ϕ' from the ξ axis, and a perfectly conducting disk as functions of polar angle θ (vertical axis) and relative rotation angle $\phi - \phi'$ (horizontal axis) at a range $L/z_a = 1$.

This work performed under the auspices of the U.S. Department of Energy by Lawrence Livermore National Laboratory under Contract DE-AC52-07NA27344.

3. References

[1] T. Rao and X. Chen. Analysis of the time reversal operator for a single cylinder under two dimensional settings. J. Electromagn. Waves Appl., 20(15):2153–2165, 2006.

[2] G. Dassios and R. Kleinman. Low Frequency Scattering. Clarendon Press, Oxford, 2000.

[3] H. Ammari and H. Kang. Reconstruction of Small Inhomogeneities from Boundary Measurements. Springer-Verlag, Berlin, 2004.

[4] D. H. Chambers. Target characterization using time-reversal symmetry of wave propagation. Int. J. Mod. Phys. B, 21:3511–3555, 2007.

[5] D. H. Chambers and J. G. Berryman. Target characterization using decomposition of the time-reversal operator: electromagnetic scattering from small ellipsoids. Inverse Problems, 22:2145–2163, 2006.